JOURNAL OF
CELLULAR
PLASTICS

Original article

Journal of Cellular Plastics
2025, Vol. 61(1) 21–35

DOI: 10.1177/0021955X241281672
journals.sagepub.com/home/cel
Sage

Evaluation of critical process parameter on the production of sustainable bead foams based on polylactic acid

Christian Brütting[1], Sarah Klotz[1] and Holger Ruckdäschel[1,2]

Abstract

A commercial grade of polylactic acid (PLA) was foamed without using modifiers to obtain expanded polylactic acid bead foams (EPLA). Typically, the foaming process is influenced by both melt properties and crystallization behavior. While factors like water temperature, die structure, and die temperature are known to have effects on bead foam processing, these aspects have not been thoroughly explored in the context of PLA bead foam production. To address this gap, a comprehensive investigation was undertaken, varying water temperature, die structure, and die temperature to discern their impact on PLA processing behavior. Results revealed that water temperature significantly influenced foaming behavior, particularly at elevated temperatures near the glass transition of PLA. Additionally, the study demonstrated that die size wielded a notable influence on all foam properties, dictating process limits. With the selection of an appropriate die size, the die temperature could be manipulated within the range of 190°C to 160°C, revealing a substantial impact on the overall process. Remarkably, the lowest densities achieved were 63 kg/m^3 with an average cell size of 36 µm and a cell density of 1.1*10^7 cells per cm^3.

Keywords

Sustainability, bead foam, PLA, bio foam, sustainable bead foam, sustainable foam

[1]Department of Polymer Engineering, University Bayreuth, Bayreuth, Germany
[2]Bavarian Polymer Institute and Bayreuth Institute of Macromolecular Research, University of Bayreuth, Bayreuth, Germany

Corresponding author:
Holger Ruckdäschel, Department of Polymer Engineering, University Bayreuth, Universitätsstraße 30, Bayreuth 95447, Germany.
Email: ruckdaeschel@uni-bayreuth.de

Introduction

Bead foams play a vital role in diverse industries, including sports, construction, and transportation, with expandable polystyrene and expanded polypropylene emerging as market leaders. In the last decades, there have been several studies dealing with new bead foams[1] such as expanded polybutylene terephthalate,[2] expanded polycarbonate,[3,4] expanded polylactide,[5–7] expanded polyamide[8] of expanded poly(ether-block-amide).[9] An overview of all developments is given by Kuhnigk et al.[1] Notably, the processing of these bead foams can be accomplished through various methods, such as autoclaving and foam extrusion. Bead foam extrusion is a continuous process that enables cost-effective processing of bead foams. However, few studies on processing behavior have been conducted to date.

Several properties significantly influence foaming behavior, with the melting[10–14] and crystallization behaviors[15–17] notably impacting density and morphology. Despite the acknowledged importance of these factors, bead foam extrusion itself remains inadequately studied and not fully understood. Only a handful of researchers have delved into the influence of process parameters on foam density and morphology.

In the exploration of bead foam extrusion, Standau et al.[2] experimented with varying throughput for EPBT, revealing that higher throughput correlates with elevated pressure profiles, increased cell nucleation, and a reduced cell size distribution. Additionally, the variation of water temperature was investigated for ETPU[18] and EPBT,[2] uncovering insights into density reduction with increased water temperature, particularly evident in EPBT at 80°C. Limited studies have been conducted on bead foam extrusion for EPP[19] and EPC.[3] For EPP,[19] the impact of temperature and blowing agents on density was explored, highlighting the role of isobutane in achieving lower densities and processing temperatures compared to CO_2. In contrast, studies on EPC focused on mechanical properties without delving into the intricacies of the process, indicating a gap in understanding concerning processing conditions like the die temperature. A recently published work[20] was dealing with PLA and PLA PHBV Blend bead foams. There the study was focused on the impact of the blend partner on the foaming behavior. It was show, that the addition of PHBV reduced the overall viscosity and changed the crystallization behavior. This resulted into an increase in bead density and a change in cell structure which is depending on the material composition.

Despite the amount of research in the field of bead foams, it is interesting to note that there is limited work on bead foam extrusion, especially of PLA. PLA is a bio-based and biodegradable polymer with a low carbon footprint[21] and therefore has a high potential to be an alternative to fossil bead foams such as EPS. However the foaming pf PLA is quite well understood, especially the influencing parameters have been analysed widely. The foaming in general is depending on various parameters which are affecting each other.[22] However the properties of PLA which are relevant for foaming have been investigated. For using PLA one should always consider the ratio of D and – lactide since this determines the crystallization properties of PLA. In addition the D-content affects the

solubility of CO2 and the interfacial tension.[23,24] Both the D-lactide and the CO2 content affect the crystallization[16,25–28] as well as the chain architecture.[29,30] It is well known, that modifications such as epoxybased modifiers can induced a branched structure which leads to higher melt properties and improve the foam structure.[31,32]

In an extrusion process at a nustell, no EPLA bead foam was created, and the factors influencing this outcome remain unknown. The research will focus on examining how the water temperature, die geometry, and die temperature affect the foam's morphology, while keeping other influencing factors consistent.

Experimental

Materials

PLA 2003D with a D-lactide content of 4.3 % from NatureWorks Ltd (Minnetonka, MN, USA) was used in this study. The glass transition is this material is at 60°C and the melting peak at 150°C.[33] The molecular weight is 232 000 g/mol with a PDI of 1.73. To create PLA foams, CO_2 was used as blowing agent.

Methods

Bead foam processing. The material was processed in a tandem extrusion line (Dr Collin GmbH, Ebersberg, Germany) consisting out of a twin-screw extrusion (L/D = 42, with a screw diameter of 25 mm) followed by a single screw extrusion line (L/D = 30, with a screw diameter of 45 mm). The blowing agent is introduced in the twin screw extruder using a Maximator "DSD500/20/SS-Edelstahl" (Maximator, Nordhausen, Germany). To produce bead foams an underwater granulation unit (UWG) (LPU MAP 5, Gala Kunststoff-und Kautschukmaschinen GmbH, Xanten, Germany) is attached. During processing a CO_2 content of 6 wt.-% was used at a knife speed of 2500 r/min. The water temperature was varied between 35°C and 55°C and two different die diameters of 2.8 mm and 1.4 mm have been used. The die temperature was varied step by step from 190°C to 160°C in steps of 10 K.

Foam analysis. The bead foam density was analyzed according to the Archimedes principle using a density balance (Mettler Toledo, Columbus, US) for 10 beads for each process condition.

To investigate the morphology of the foamed samples, scanning electron microscopy was used (JOEL Ltd, Welwyn Garden City, UK). The samples have been cut with a razor blade, and a sputter coated 1.3 nm thick gold layer. The resulting images were analyzed using ImageJ. The cell density and nucleating density were calculated in accordance to other publications[33,34]

The melting behavior has been analyzed using a DSC (DSC1, Mettler Toledo, Columbus, US). Depending on the density, a sample weight of 2 – 6 mg was analyzed. The samples have been heated from 25°C to 200°C at a heating rate of 10 K/min under a N_2

atmosphere to evaluate the influence of the processing conditions on the thermal properties.

Results and discussion

Initially, the impact of water temperature is assessed, succeeded by an examination of die size and die temperature. The setup was held constant, ensuring a systematic investigation of each selected parameter on the process.

Influence of water temperature

Bead foams undergo cutting and stabilization with water serving as the cooling medium. The expansion, crystallization, and cooling of particles occur concurrently, with water temperature playing a crucial role in the stabilization of particle foams.[2] The temperature of the water is adjusted within the range of 35°C (the lowest achievable temperature) and 55°C (5 K below the glass transition temperature, Tg, of PLA). A comprehensive summary of the processing parameters and resulting densities is presented in Table 1.

The analysis of the process parameters indicates that the water temperature does not exhibit a recognizable impact on the melt temperature. However, it is noteworthy that lower temperatures coincide with higher pressures. The constancy of temperature influence was maintained for a minimum of 30 min, ruling out process variations as the cause of pressure changes. An intriguing hypothesis is that the process water may cool the melt at the die plate. Notably, the pressure of the melt remains unchanged until the water temperature falls below 45°C. This observation suggests that, above this temperature, cooling beneath the glass transition temperature induces partial solidification of the melt, resulting in a subsequent pressure increase.

The bead morphology is used to quantify the effect of water temperature on cell structure. The variation of these properties (density, cell size, cell density and nucleation density) as a function of water temperature is shown in Figure 1. The corresponding SEM images and cell distributions are summarized in Figure 2.

At the lowest achievable water temperature of 35°C, the particles exhibit an average density of approx. 220 kg/m^3. As the temperature increases, the average density decreases

Table 1. Overview of relevant foaming parameter at varying water temperatures.

Water temperature/°C	Melt temperature/°C	Pressure at die plate/Bar	Density/Kg/m^3
35	155	155	218 ± 21
40	155	155	188 ± 18
45	155	148	231 ± 19
50	155	149	153 ± 14
55	155	149	301 ± 24

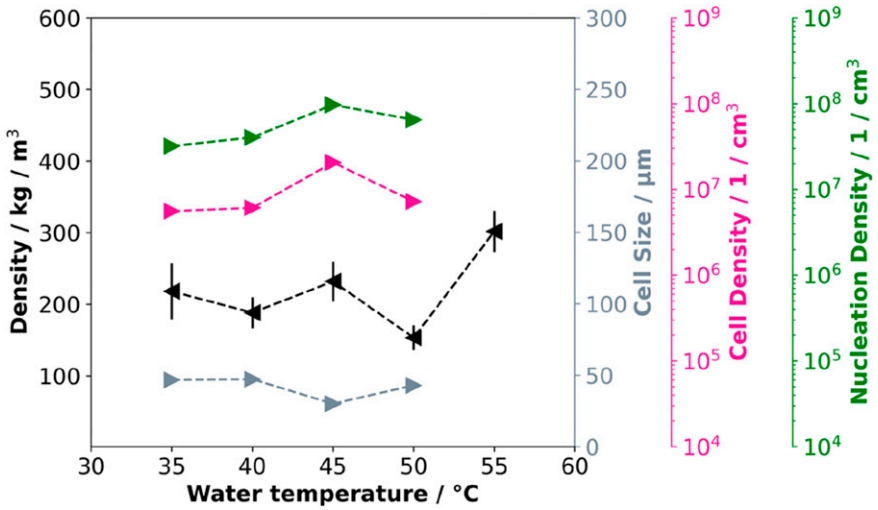

Figure 1. Density, cell size, cell density, and nucleation density as a function of water temperature.

slightly up to a water temperature of 45°C. At higher temperatures than 50°C, a notable increase in density is observed and the process becomes unstable.

The increase in density at high temperatures (above 50°C) is due to insufficient foam stabilization which leads to shrinkage after expansion. Additionally, the elevated temperature enhances the diffusivity of the blowing agent, leading to its loss at the bead surface. Thus the blowing agent contributes less to the expansion. At a water temperature of 50°C, the beads stabilize more rapidly, leading to lower densities. Temperatures below 50°C yield densities at approx. 230 kg/m^3, as the particles are cooled below the glass transitions more quickly, ensuring foam stabilization.

In addition to density, cell growth and stabilization are affected by temperature. Up to 50°C, the average cell size of all particles remains below 50 µm, indicating that water temperature has no significant effect on cell formation in the examined range. Above 50°C, the cell size distribution was not determined because it is very inhomogeneous with comparatively large cells. SEM Images for all particles are shown in Figure 2.

The glass transition temperature of PLA is approx. 60°C, and at 55°C insufficient stabilization occurs and cell coalescence takes place. This is due to the remaining CO_2 which lowers the glass transition temperature and thus prevents stabilization. The influence of CO_2 on the glass transition temperature has already been shown in several papers.[35–37] Here, even small amounts of CO_2 can lead to a significant decrease in the glass transition temperature and delay stabilization in the manufacturing process. The CO_2 desorbs rapidly after leaving the die, resulting in lower concentrations during stabilization. The CO_2 content during the foaming process varies, depending on the bead volume, the temperatures distribution and the dissolved CO_2. Unfortunately, it's not possible to measure the CO_2 content during processing. For an estimate, to realize a glass transition temperature of 50°C in the PLA, a CO_2 content of about 1.5 % must be

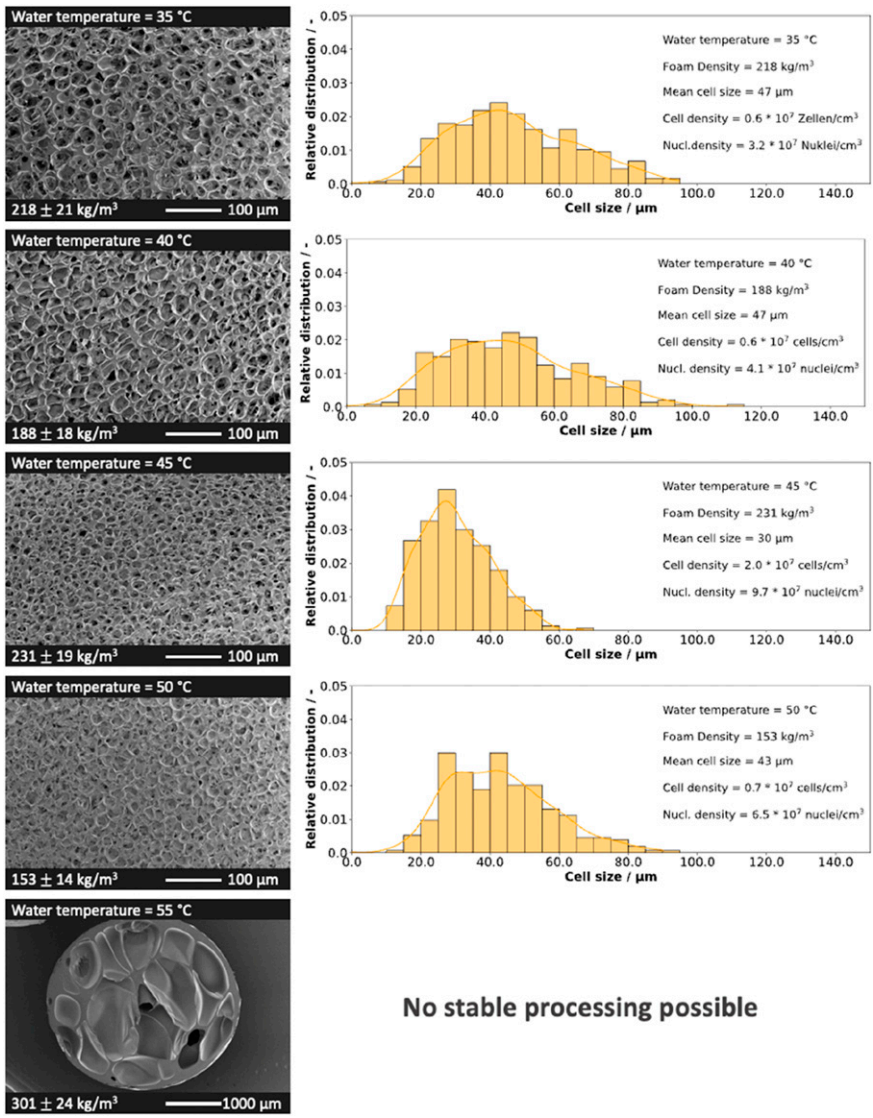

Figure 2. SEM images of PLA bead foams and the cell size distribution at varying water temperatures.

present.[35] The cell and nucleation densities exhibit an increase with temperature, a phenomenon attributable to the lower solubility resulting from generally elevated temperatures. The higher temperature causes the particles to cool more slowly, which decreases solubility and promotes nucleation. The cell size distribution of the investigated particles is summarized in Figure 2, together with all morphological characteristics.

A change in water temperature leads to varying thermal characteristics. To investigate these impact, the bead foams were analyzed by DSC for their melting behavior at the different conditions. Figure 3 illustrates the cold crystallization, enthalpy of fusion, and total enthalpy plotted against water temperature, providing insights into the thermal characteristics and crystallization patterns associated with the changing conditions.

No clear trend is observed for total melting enthalpy versus water temperature. However, low melting enthalpies occur at low (35°C and 40°C) and high temperatures (55°C) and no crystallization was found for the unfoamed material[33] in DSC measurements. Due to the significantly faster cooling of the polymer melt in the UWG (Underwater granulation), crystallization during processing is not expected.

In this context, crystallization is likely influenced by CO2 or strain-induced mechanisms. Past studies have demonstrated that CO2 enhances the crystallization kinetics of PLA,[25,26] with the specific kinetics affected by factors such as blowing agent type, cooling rate, and concentration.[38] In addition, CO2 lowers the glass transition temperature[16,27,28,35,39] and crystallization temperature.[16,25–28]

Research on foam extrusion in the presence of CO2 has explored strain-induced crystallization, indicating that an increased strain rate promotes crystal formation and growth.[26] Additionally, previous findings for PLA by Takada et al.[27] suggest that CO2 has a dual effect: reducing crystallite nucleation while enhancing growth rate. Due to a constant die setup, a change in strain rate can be excluded, indicting the influence of CO2 and cooling as major driving forces in changing the crystallinity.

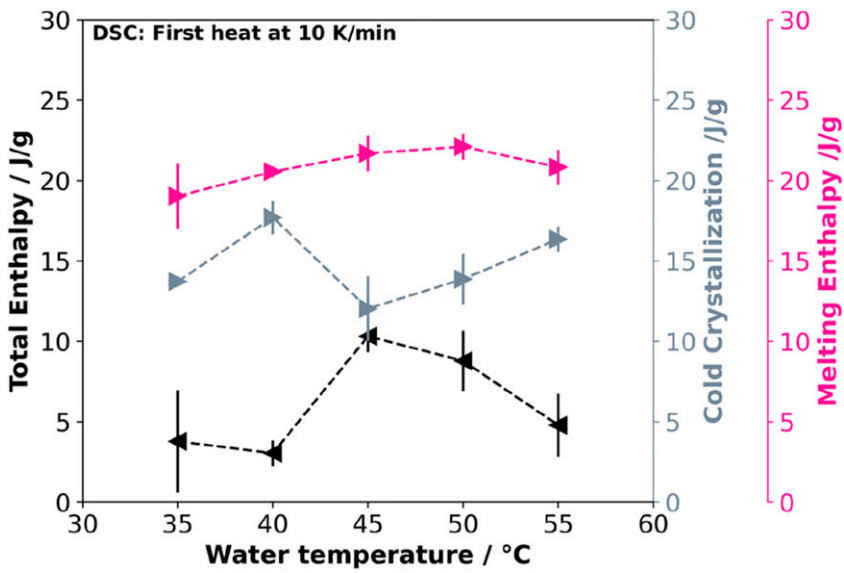

Figure 3. Analysis of melt and crystallization enthalpies depending on different water temperatures during manufacturing.

The cooling rate influences the bead temperature and subsequently determines the diffusion rate of CO_2 which is affecting the crystallization. Additionally, the expansion of the bead induces elongational forces, leading to the formation and growth of crystallites. At ideal temperatures (here at 45°C and 50°C) sufficient mobility of the polymer chains is given to promote crystal growth leading to high crystallinities. Conversely, at lower temperatures the foam lacks the required mobility, while temperatures exceeding 50°C lead to rapid CO_2 desorption near the glass transition temperature (~60°C), preventing effective crystal growth.

Comparative analysis with other particle foams, particularly EPBT, reveals limited studies on the impact of water temperature. Unlike PBT, EPLA shows pronounced changes in crystallinity during particle production due to differing crystallization and processing behaviors. The faster crystallization of PBT underlines the differences between EPLA and EPBT in bead foam production.[2,40] Due to the low crystallization speed of PLA, influences from cooling processes in the UWG can influence the properties, which is why the evaluation of crystallinity can not be fully attributed to the properties directly during the production. For this reason the crystallization will not be analysed in detail in the upcoming chapters. However the results are display as supplementary informations.

Influence of die geometry

Owing to variations in die diameter, the particles exhibit distinct mass and size distributions. This discrepancy extends to the cooling behavior during foaming, impacting the formation of the cell structure and, consequently, the resulting density. Remarkably, there is a lack of published literature addressing the influence of diverse die geometries in a bead foam extrusion process. The diverse setups and process parameters are comprehensively detailed in Table 2. Further insights into particle characteristics are depicted in Figure 4, encompassing SEM images, cell size distribution, and morphological parameters, including density, cell size, and cell density.

Here it needs to be mentioned, that the throughput must be adapted from 6.5 kg/h at a die diameter of 1.4 mm to 8 kg/h with a die with 2.8 mm in diameter.

Particles produced with the larger die exhibit a average density of 230 kg/m^3, whereas beads observed from the smaller die have an average density of 170 kg/m^3. This disparity arises from their higher mass due to the prolonged cooling time of larger particles. Consequently, these particles may not undergo sufficient stabilization. The cell size distribution of both bead foams is equal to a Gaussian normal distribution.

Table 2. Overview of relevant foaming parameter at varying die geometries.

Die diameter/mm	Melt temperature/°C	Pressure at die plate/Bar	Density/Kg/m^3
2 x ϕ 1.4	156	157	170 ± 24
1 x ϕ 2.8	156	157	230 ± 23

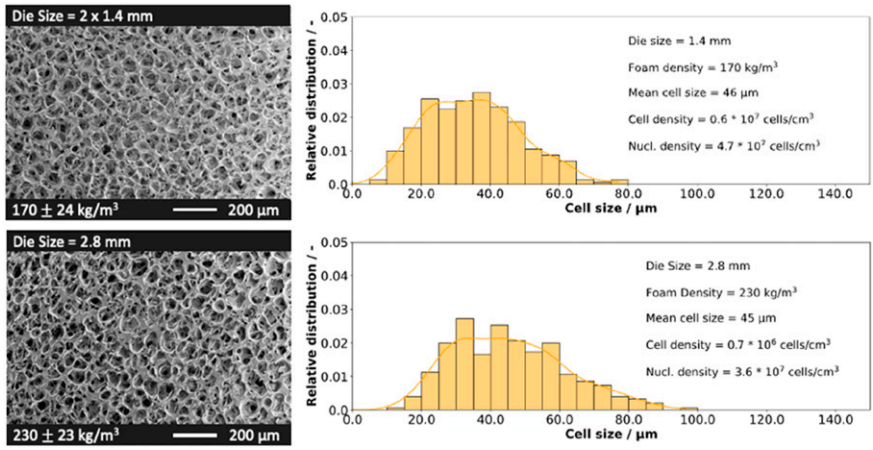

Figure 4. SEM images of PLA bead foams and the cell size distribution at varying die geometries.

The bead foam produced with the larger die (2.8 mm diameter) shows an average cell size of 45 µm. Similarly, particles from the smaller dies (1.4 mm diameter) have an average cell size of 46 µm. However, differences in cell density and nucleation density are observed. Specifically, particles from the smaller dies exhibit a cell density 10 times higher, maintaining a comparable nucleation density in comparison to the larger die setup. These differences can be attributed to the extended cooling time required for larger particles, leading to more pronounced cell coalescence and consequently a reduced cell count.

The trials revealed that the die temperature could be more precisely adjusted with a 2.8 mm diameter die. Consequently, this configuration is used in the subsequent investigation focusing on the influence of die temperature.

Influence of die temperature

The temperature of the melt cannot be adjusted directly; instead, it relies on controlling temperatures at various points of the extrusion line, including the adapter, deflection head, and die plate. Notably, the die plate temperature is a decisive factor for bead foam processing as it is in direct contact with the water of the UWG system. If the die plate temperature drops to a too low value, depending on the material and the process, the melt may, potentially surpassing the system's pressure limit.

The 2.8 mm diameter die can undergo more cooling compared to the 1.4 mm die. This is attributed to the larger mass of polymer in the larger die, slowing down the solidification of the melt. Consequently, this allows lower die plate temperatures without disrupting the process. Identifying the potential significance of die plate temperature, it is varied f in subsequent analyses or a detailed investigation.

When varying die plate temperatures, the CO_2 content was kept constant at 6 wt%. The water temperature was set at 45°C, with no overpressure in the UWG, and the knife speed

was fixed at 2500 r/min to achieve spherical particles. Considering temperatures of 140°C in the single screw extruder, the melt temperature is estimated to be around 155°C, resulting in a die plate pressure of 157 bar. The die temperature, initially set at 190°C, was systematically reduced to 160°C. This shift in temperature imparts alterations to the pressure and temperature profiles throughout the process. The impacts of this temperature change on melt temperature, pressure upstream of the die plate, and particle density are detailed in Table 3.

As indicated in Table 3, a reduction in die plate temperature not only results in a lower melt temperature but also leads to an elevated pressure at the die plate. The lower in die plate temperature contributes to a lower melt temperature, subsequently increasing the viscosity of the melt and raising pressure levels in both the UWG and the extrusion unit.

As depicted in Table 3, a variation in die temperature significantly influences the resulting density. The temperature exerts a direct and indirect effect on the particles. Reducing the temperature accelerates melt solidification after extrusion in the UWG, directly impacting particle expansion and stabilization. Simultaneously, this temperature reduction indirectly increases the process pressure, resulting in increased solubility. This intensified thermodynamic imbalance elevates the gas release rate, affecting both cell formation and expansion. The changes in morphology of individual beads are shown in Figure 5, where the SEM images of the beads are compared. The morphology is further analyzed using histograms, considering cell sizes, cell densities, and nucleation densities, all of which are correlated to the indicated density.

As the temperature decreases, there is a simultaneous decrease in densities and cell sizes, while cell densities and nucleation densities increase with decreasing die temperature - except at 160°C. At a die temperature of 190°C, the particle morphology maintains an average cell size of 45 µm. The trend shifts as the die temperature decreases, showcasing a decrease in average cell size: 41 µm at 180°C, 38 µm at 170°C, and 36 µm at 160°C. This phenomenon can be attributed to an increased viscosity of the melt at lower temperatures, resulting in increased pressures and decreased diffusion rates. As the die temperature decreases, the elevated viscosity leads to higher pressures, fostering stronger nucleation of cells and, consequently, an increase in nucleation density. Similar trends have been shown in literature for a variation in temperature for extrusion foams.[41] Simultaneously, the lower diffusion rates slow down CO2 desorption, prolonging its contribution to expansion as the polymer melt remains plasticized for an extended

Table 3. Overview of relevant foaming parameters.

Die plate temperature/°C	Melt temperature/°C	Pressure at die plate/Bar	Density/Kg/m^3
190	156	157	230 ± 23
180	153	165	214 ± 7
170	152	173	186 ± 11
160	151	191	63 ± 3

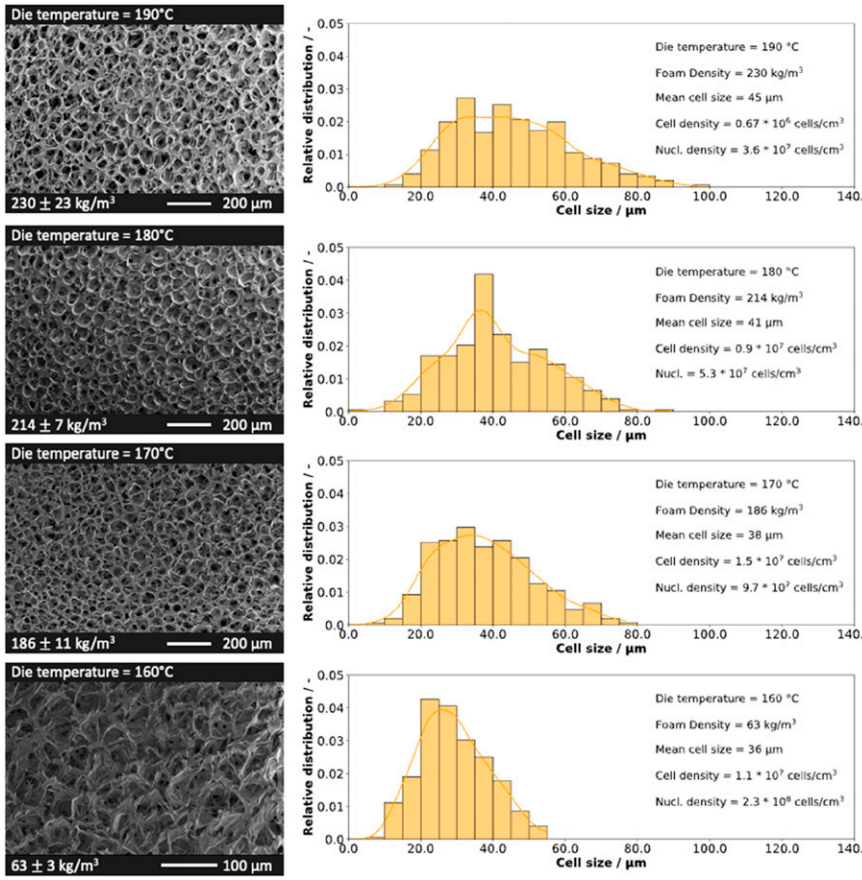

Figure 5. SEM images of PLA bead foams and the cell size distribution at varying die temperatures.

duration.[32,42] Furthermore, the coupling between higher melt viscosity and increased melt strength counteracts cell coalescence, ultimately leading to higher cell densities.

Conclusion

In this investigation, bead foams based on PLA were produced to investigate the impact of processing conditions, including water temperature, die geometry, and die temperature. The change of water temperature strongly influences foam properties. Excessive temperatures led to cell coalescence, resulting in elevated density. Conversely, lower temperatures facilitated foam stabilization, yielding densities around 200 kg/m³. Changes in die geometry necessitated adjustments in throughput to ensure consistent process conditions. Notably, an increased diameter leads to lower densities and larger cell sizes. This

trend is ascribed to the increasedthermal mass of the beads, extending the time for cell growth. Consequently, density decreased, and cell coalescence ensued. Of all the variables studied, the die temperature exhibited the most pronounced effect on foam properties. A transition from 190 to 160°C led to a substantial reduction in foam density from 230 kg/m³ to 63 kg/m³. Simultaneously, this temperature shift resulted in a decrease in cell size and an increase in cell density as well as nucleation density. Lowering the die temperature increased the pressure profile, reducing gas losses at the die, and promoting higher nucleation rates. Moreover, the lower temperature facilitated stabilization, mitigating cell coalescence and reducing cell size to approximately 36 µm.

This study emphasizes the importance and impact of selected parameters on the bead foam extrusion. Transferability to other bead foam related topics is given since the material was not varied. In future, the findings can be used to steer the process and combine the knowledge of material and process based literatures.

Acknowledgments

The authors would like to acknowledge Bavarian Polymer Institute (BPI) for providing access to different analysis methods. Furthermore, we would like to thank Sebastian Gröschel and Annika Pfaffenberger for their support in preparing and analyzing the samples.

Author contributions

Christian Brütting: conceptualization, writing, reviewing, and editing sections, Sarah Klotz: reviewing, and editing sections. Prof. Dr.-Ing. Holger Ruckdäschel: supervision, reviewing and editing sections.

Declaration of conflicting interests

The author(s) declared no potential conflicts of interest with respect to the research, authorship, and/or publication of this article.

Funding

The author(s) disclosed receipt of the following financial support for the research, authorship, and/or publication of this article: This research was funded by German Research Foundation (DFG), Grant No. AL474/ 34-1

ORCID iD

Holger Ruckdaschel https://orcid.org/0000-0001-5985-2628

Supplemental Material

Supplemental material for this article is available online.

References

1. Kuhnigk J, Standau T, Dörr D, et al. Progress in the development of bead foams – a Review. *J Cell Plast* 2022; 58(4): 707–735. DOI: 10.1177/0021955X221087603.
2. Standau T, Hilgert K, Kuhnigk J, et al. Influence of processing conditions on the Appearance of bead foams made of the Engineering Thermoplastic polybutylene terephthalate (E-PBT). In SPE Foams 13.-16. September 2021 Virtual Conference, 2021.
3. Weingart N, Raps D, Kuhnigk J, et al. Expanded polycarbonate (EPC)—a new Generation of high-temperature Engineering bead foams. *Polymers* 2020; 12(10): 2314. DOI: 10.3390/polym12102314.
4. Sánchez-Calderón I, Bernardo V, Martín-de-León J, et al. Novel Approach based on Autoclave bead foaming to produce expanded polycarbonate (EPC) bead foams with Microcellular structure and controlled crystallinity. *Mater Des* 2021; 212: 110200. DOI: 10.1016/j.matdes.2021.110200.
5. Nofar M, Ameli A and Park CB. Development of polylactide bead foams with Double crystal melting peaks. *Polymer* 2015; 69(1): 83–94. DOI: 10.1016/j.polymer.2015.05.048.
6. Brütting C, Dreier J, Bonten C, et al. Amorphous polylactide bead foam–effect of Talc and chain extension on foaming behavior and compression properties. *J. Renew. Mater* 2021; 9(11): 1859–1868. DOI: 10.3260/jrm.2021.016244.
7. Dreier J, Brütting C, Ruckdäschel H, et al. Investigation of the thermal and hydrolytic degradation of polylactide during autoclave foaming. *Polymers* 2021; 13(16): 2624. DOI: 10.3390/polym13162624.
8. Dörr D, Raps D, Kirupanantham D, et al. Expanded polyamide 12 bead foams (EPA) Thermo-mechanical properties of Molded Parts. *AIP Conf Proc* 2020; 1: 020037. DOI: 10.1063/1.5142952.
9. Jiang J, Liu F, Chen B, et al. Microstructure development of PEBA and its impact on Autoclave foaming behavior and Inter-bead Bonding of EPEBA beads. *Polymer* 2022; 256: 125244. DOI: 10.1016/j.polymer.2022.125244.
10. Spitael P and Macosko CW. Strain Hardening in polypropylenes and its role in extrusion foaming. *Polym Eng Sci* 2004; 44(11): 2090–2100. DOI: 10.1002/pen.20214.
11. Jahani Y and Barikani M. Effect of blend composition on extrusion foaming Behaviour of linear and branched polypropylene Ternary blends. *Iranian Polymer Journal*. 2007.
12. Wan C, Sun G, Gao F, et al. Effect of phase compatibility on the foaming behavior of LDPE/HDPE and LDPE/PP blends with Subcritical CO2 as the blowing agent. *J Supercrit Fluids* 2017; 120: 421–431. DOI: 10.1016/j.supflu.2016.05.038.
13. Bahreini E, Aghamiri SF, Wilhelm M, et al. Influence of molecular structure on the Foamability of polypropylene: Linear and extensional rheological fingerprint. *J Cell Plast* 2018; 54(3): 515–543. DOI: 10.1177/0021955X17700097.
14. Corre YM, Maazouz A, Duchet J, et al. Batch foaming of chain extended PLA with Supercritical CO2: influence of the Rheological properties and the process parameters on the Cellular structure. *J Supercrit Fluids* 2011; 58(1): 177–188. DOI: 10.1016/j.supflu.2011.03.006.
15. Nofar M. Effects of Nano-/micro-sized additives and the corresponding induced crystallinity on the extrusion foaming behavior of PLA using Supercritical CO2. *Mater Des* 2016; 101: 24–34. DOI: 10.1016/j.matdes.2016.03.147.

16. Li D, Liu T, Zhao L, et al. Foaming of Poly(Lactic acid) based on its Nonisothermal crystallization behavior under Compressed carbon Dioxide. *Ind Eng Chem Res* 2011; 50(4): 1997–2007. DOI: 10.1021/ie101723g.
17. Ren Q, Wang J, Zhai W, et al. Solid state foaming of Poly(Lactic acid) Blown with Compressed CO2 : influences of Long chain branching and induced crystallization on foam expansion and cell morphology. *Ind Eng Chem Res* 2013; 52(37): 13411–13421. DOI: 10.1021/ie402039y.
18. Shabani A, Fathi A, Erlwein S, et al. Thermoplastic polyurethane foams: from Autoclave Batch foaming to bead foam extrusion. *J Cell Plast* 2021; 57(4): 21–411. DOI: 10.1177/0021955X20912201.
19. Tammaro D, Ballesteros A, Walker C, et al. Expanded beads of high melt strength polypropylene Moldable at low Steam pressure by foam extrusion. *Polymers* 2022; 14(1): 205. DOI: 10.3390/polym14010205.
20. Brütting C, Dreier J, Bonten C, et al. Biobased Immiscible polylactic acid (PLA): Poly(3-Hydroxybutyrate-Co-3-Hydroxyvalerate) (PHBV) blends: impact of rheological and non-isothermal crystallization on the bead foaming behavior. *J Polym Environ* 2024; 32(3): 4182–4195. DOI: 10.1007/s10924-024-03186-9.
21. Standau T, Zhao C, Murillo Castellón S, et al. Chemical modification and foam processing of polylactide (PLA). *Polymers* 2019; 11(2): 306. DOI: 10.3390/polym11020306.
22. Nofar M and Park CB. Poly (lactic acid) foaming. *Prog Polym Sci* 2014; 39(10): 1721–1741. DOI: 10.1016/j.progpolymsci.2014.04.001.
23. Mahmood SHH, Ameli A, Hossieny N, et al. The interfacial tension of Molten polylactide in supercritical carbon dioxide. *J Chem Thermodyn* 2014; 75: 69–76. DOI: 10.1016/j.jct.2014.02.017.
24. Mahmood SH, Keshtkar M and Park CB. Determination of carbon dioxide solubility in polylactide acid with accurate PVT properties. *J Chem Thermodyn* 2014; 70: 13–23. DOI: 10.1016/j.jct.2013.10.019.
25. Naguib HE, Park CB and Song SW. Effect of Supercritical gas on crystallization of linear and branched polypropylene Resins with foaming Additives. *Ind Eng Chem Res* 2005; 44(17): 6685–6691. DOI: 10.1021/IE0489608/ASSET/IMAGES/LARGE/IE0489608F00012.JPEG.
26. Tabatabaei A and Park CB. In-situ Visualization of PLA crystallization and crystal effects on foaming in extrusion. *Eur Polym J* 2017; 96(June): 505–519. DOI: 10.1016/j.eurpolymj.2017.09.026.
27. Takada M, Hasegawa S and Ohshima M. Crystallization kinetics of Poly (L-lactide) in contact with Pressurized CO2. *Polym Eng Sci* 2004; 44(1): 186–196. DOI: 10.1002/pen.20017.
28. Takada M, Tanigaki M and Ohshima M. Effects of CO2 on crystallization kinetics of polypropylene. *Polym Eng Sci* 2001; 41(11): 1938–1946. DOI: 10.1002/pen.10890.
29. Yu L, Toikka G, Dean K, et al. Foaming Behaviour and cell structure of Poly (Lactic acid) after various modifications. *Polym Int* 2013; 62(5): 759–765. DOI: 10.1002/pi.4359.
30. Chen P, Wang W, Wang Y, et al. Crystallization-induced Microcellular foaming of poly (lactic acid) with high volume expansion ratio. *Polym Degrad Stab* 2017; 144: 231–240. DOI: 10.1016/j.polymdegradstab.2017.08.022.
31. Mihai M, Huneault MA and Favis BD. Rheology and extrusion foaming of chain-branched Poly(Lactic acid). *Polym Eng Sci* 2010; 50(3): 629–642. DOI: 10.1002/pen.21561.

32. Wang J, Zhu W, Zhang H, et al. Continuous processing of low-density, Microcellular Poly(Lactic acid) foams with controlled cell morphology and crystallinity. *Chem Eng Sci* 2012; 75: 390–399. DOI: 10.1016/j.ces.2012.02.051.
33. Brütting C, Dreier J, Bonten C, et al. Sustainable Immiscible polylactic acid (PLA) and Poly(3-Hydroxybutyrate- Co -3-Hydroxyvalerate) (PHBV) blends: crystallization and foaming behavior. *ACS Sustainable Chem Eng* 2023; 11(17): 6676–6687. DOI: 10.1021/acssuschemeng.3c00199.
34. Okolieocha C, Raps D, Subramaniam K, et al. Microcellular to Nanocellular polymer foams: Progress (2004-2015) and future Directions - a Review. *Eur Polym J* 2015; 73: 500–519. DOI: 10.1016/j.eurpolymj.2015.11.001.
35. Brütting C, Dreier J, Bonten C, et al. Glass transition of PLA-CO 2 Mixtures after Solid-State Saturation. *J Cell Plast* 2022; 58(6): 917–931. DOI: 10.1177/0021955X221144543.
36. Nofar M, Zhu W and Park CB. Effect of dissolved CO2 on the crystallization behavior of linear and branched PLA. *Polymer* 2012; 53(15): 3341–3353. DOI: 10.1016/j.polymer.2012.04.054.
37. Ding W, Chu RKM, Mark LH, et al. Non-isothermal crystallization behaviors of Poly (Lactic Acid)/cellulose nanofiber composites in the presence of CO2. *Eur Polym J* 2015; 71: 231–247. DOI: 10.1016/j.eurpolymj.2015.07.054.
38. Nofar M, Tabatabaei A, Ameli A, et al. Comparison of melting and crystallization behaviors of polylactide under high-pressure CO2, N2, and He. *Polymer* 2013; 54(23): 6471–6478. DOI: 10.1016/j.polymer.2013.09.044.
39. Chiou JS and Paul DR. Effects of CO2 Exposure on gas Transport properties of Glassy polymers. *J Memb Sci* 1987; 32(2–3): 195–205. DOI: 10.1016/S0376-7388(00)85006-1.
40. Kuhnigk J, Krebs N, Standau T, et al. Evaluation of the fusion Quality of bead foams made from polybutylene terephthalate (E-PBT) depending on the processing temperature. *Macromol Mater Eng* 2022; 307(11): 2200419. DOI: 10.1002/MAME.202200419.
41. He M and Hu S. A Strategy for extending the processing temperature for polypropylene in foam extrusion and its Theoretical Validation. *J Cell Plast* 2023; 59(4): 293–312. DOI: 10.1177/0021955X221144705.
42. Naguib HE, Park CB, Panzer U, et al. Strategies for achieving Ultra low-density polypropylene foams. *Polym Eng Sci* 2002; 42(7): 1481–1492. DOI: 10.1002/pen.11045.